



A unique xylose reductase from *Thermomyces lanuginosus*: Effect of lignocellulosic substrates and inhibitors and applicability in lignocellulosic bioconversion

Meng Zhang^a, Adarsh Kumar Puri^{a,*}, Zhengxiang Wang^b, Suren Singh^a, Kugen Permaul^a

^a Department of Biotechnology and Food Technology, Durban University of Technology, Durban, South Africa

^b Key Laboratory of Industrial Fermentation Microbiology of Ministry of Education, Tianjin University of Science and Technology, Tianjin 300457, China

ARTICLE INFO

Keywords:

Xylose reductase
Lignocellulose
Thermomyces lanuginosus
Ferulic acid
Xylitol

ABSTRACT

In this study, the xylose reductase gene (*XRTL*) from *Thermomyces lanuginosus* SSBP was expressed in *Pichia pastoris* GS115 and *Saccharomyces cerevisiae* Y294. The purified 39.2 kDa monomeric enzyme was optimally active at pH 6.5 and 50 °C and showed activity over a wide range of temperatures (30–70 °C) and pH (4.0–9.0), with a half-life of 1386 min at 50 °C. The enzyme preferred NADPH as cofactor and showed broad substrate specificity. The enzyme was inhibited by Cu²⁺, Fe²⁺ and Zn²⁺, while ferulic acid was found to be the most potent lignocellulosic inhibitor. Recombinant *S. cerevisiae* with the *XRTL* gene showed 34% higher xylitol production than the control strain. *XRTL* can therefore be used in a cell-free xylitol production process or as part of a pathway for utilization of xylose from lignocellulosic waste.

1. Introduction

With annual global production exceeding 200 billion tons, lignocelluloses are the most abundant biomass on planet Earth (Jiang et al., 2018). The last decade has witnessed growing research interest towards exploitation of lignocellulosic biomass for production of several value-added compounds (Rao et al., 2016). Most of the research has been focused on conversion of the recalcitrant lignocellulosic biomass into viable products. Although chemical methods are economical, manipulation of the enzymatic machinery of microbial systems for enhanced bioconversion of lignocellulosic biomass is preferred due to its environment-friendly nature and for long-term sustainability.

The pentose sugar, xylose, constitutes a major part of the lignocellulosic hemicellulose and has the potential for production of several value-added compounds. Xylitol, a low-calorie sugar substitute in food, pharmaceuticals, nutraceuticals, and beverage industries, is one such product with an annual market of USD 340 million per year, and expected to reach USD 670 million by 2020 (Medina et al., 2018). Current production of industrial xylitol is expensive and energy-intensive which requires pure xylose and high temperature and pressure for catalytic hydrogenation. Although biotechnological production of xylitol is cost-effective and uses milder conditions, there are only a few microorganisms that can metabolize xylose, and that too with poor efficiency and yield.

Microbial xylose reductases (EC 1.1.1.21) initiate the first step of xylose metabolism, catalyzing the reduction of xylose to xylitol, and its properties affect efficiency of xylose fermentation (Kratzer et al., 2006). The enzyme belongs to the aldo-keto reductase (AKR) super family, commonly found in yeasts and filamentous fungi. Xylose reductase has attracted significant scientific attention due to its application in the fermentation of lignocellulosic biomass to ethanol and xylitol. Although the use of lignocellulosic biomass for bioconversion of xylose to xylitol using xylose reductase is promising, there is a lack of knowledge on the effect of several lignocellulose-derived phenolic and non-phenolic by-products produced during pretreatment processes. Therefore, it is crucial to characterize xylose reductases from microorganisms to explore maximum efficiency of bioconversion of xylose into value-added products such as polyols or ethanol. Genome and secretome analysis of the thermophilic filamentous fungus *Thermomyces lanuginosus* has revealed several enzymes of industrial importance (Mchunu et al., 2013). This study was aimed at expressing a novel xylose reductase from *T. lanuginosus*, characterizing and investigating the effect of different inhibitors and substrates. Additionally, the enzyme was expressed in *Saccharomyces cerevisiae* to investigate its effect on xylitol production.

* Corresponding author.

E-mail address: puriadarsh@gmail.com (A.K. Puri).

<https://doi.org/10.1016/j.biortech.2019.02.102>

Received 18 December 2018; Received in revised form 21 February 2019; Accepted 22 February 2019

Available online 23 February 2019

0960-8524/ © 2019 Elsevier Ltd. All rights reserved.

2. Materials and methods

2.1. Microorganisms, plasmids and cultural conditions

The gene for xylose reductase (*XRTL*) was sourced from *T. lanuginosus* SSBP cultivated in a medium containing (w/v) 2% xylose, 0.087% K_2HPO_4 , 0.068% KH_2PO_4 , 0.02% KCl, 0.1% NH_4NO_3 , 0.02% $MgSO_4$ and 0.4% yeast extract; pH 6.0. *Escherichia coli* JM109 was used as a host for plasmid construction and cultivated in a low salt Luria–Bertani (LB) medium at 37 °C. *Pichia pastoris* GS115 (Invitrogen) and *Saccharomyces cerevisiae* Y294 (*MATa his3Δleu2Δlys2Δura3Δ*) [ATCC 201160] were used for extracellular and intracellular expression of recombinant proteins, respectively. The plasmid pPIC9K (Invitrogen) was used to express *XRTL* in *P. pastoris* while pAUR135 (Takara) was used to develop the *S. cerevisiae* integrative plasmid. *P. pastoris* was cultivated in YPD (1% yeast extract, 2% peptone, 2% glucose) medium at 30 °C while *S. cerevisiae* Y294 cultures were grown in SC minimal medium (0.67% yeast nitrogen base without amino acids, 0.2% yeast synthetic drop-out medium supplements and 2% glucose) at 30 °C.

2.2. Construction of recombinant *XRTL* expression plasmids for *P. pastoris* GS115 and *S. cerevisiae* Y294

Total RNA isolation and cDNA synthesis was performed according to Zhang et al. (2015b). The xylose reductase gene was amplified from cDNA using *XRTL*-specific (*XRTL*-P) primers. The PCR products were digested with *Eco*RI and *Xba*I, and ligated into the pPIC9K vector linearized with *Eco*RI and *Avr*II, and the construct was named *XRTL*-pPIC9K.

The *XRTL* gene was integrated into *S. cerevisiae* Y294 chromosome XV at a solo long terminal repeat site according to Flagfeldt et al. (2009). The homologous arms, promoter (*TEF1*) and terminator (*CYC1*) of the expression cassette were amplified using *S. cerevisiae* Y294 genomic DNA. The final expression plasmid (Fig. 1) was named as 19up-*TEF1*-*XRTL*-*CYC*-down-pAUR135.

2.3. Transformation of *P. pastoris* and *S. cerevisiae* with *XRTL*

The recombinant plasmids *XRTL*-pPIC9K and 19up-*TEF1*-*XRTL*-*CYC*-down-pAUR135 were linearized with *Sac*I and *Spe*I, respectively. These linearized plasmids were transformed into *P. pastoris* GS115 and *S. cerevisiae* Y294 via electroporation (Gene pulser Xcell, Bio-Rad) by following the manufacturer's protocol. Positive transformants of *P. pastoris* were selected on YPD-Geneticin plates containing Geneticin, according to the manufacturer's instructions (Invitrogen). Similarly, electroporated cells of *S. cerevisiae*, were incubated in YPD broth at 30 °C for 4 h and selected on YPD medium containing 0.5 μg/ml Aureobasidin A (Takara). Selection of pAUR135 excised clones was performed according to manufacturer's protocols (Takara). Colony PCR was then performed to identify positive clones of *P. pastoris* and *S. cerevisiae*, according to Look et al. (2011).

2.4. Production and purification of recombinant xylose reductase from *P. pastoris*

Recombinant *P. pastoris* GS115 harbouring the *XRTL* gene was cultivated in YPD medium and induced by 0.5% (v/v) methanol in BMMY medium (1% yeast extract, 2% peptone, 1.34% YNB and 4×10^{-5} % biotin in 100 mM phosphate buffer, pH 6.0) for the production of recombinant protein in shake flasks as per the manufacturer's protocol. *P. pastoris* GS115 transformed with pPIC9K was used as a control.

The recombinant *XRTL* was purified on an AKTA Purifier 100 (GE Healthcare) using classical purification steps according to Zhang et al. (2015a), using DEAE (HiTrap DEAE FF 5 ml, GE Healthcare) and gel filtration (Superdex 200 Increase 10/300 GL, GE Healthcare) columns. Homogeneity of the purified protein was estimated on SDS-PAGE gels. Protein concentration was measured using the method of Bradford (Bradford, 1976) with bovine serum albumin (BSA) as the standard. Xylose reductase activity was estimated according to Kumar and Gummadi (2011) by continuous spectrophotometric assay using commercial xylose (Sigma) as substrate and NADPH (molar extinction coefficient = 6.22 mol/l/cm) as a reductant. One enzyme unit was

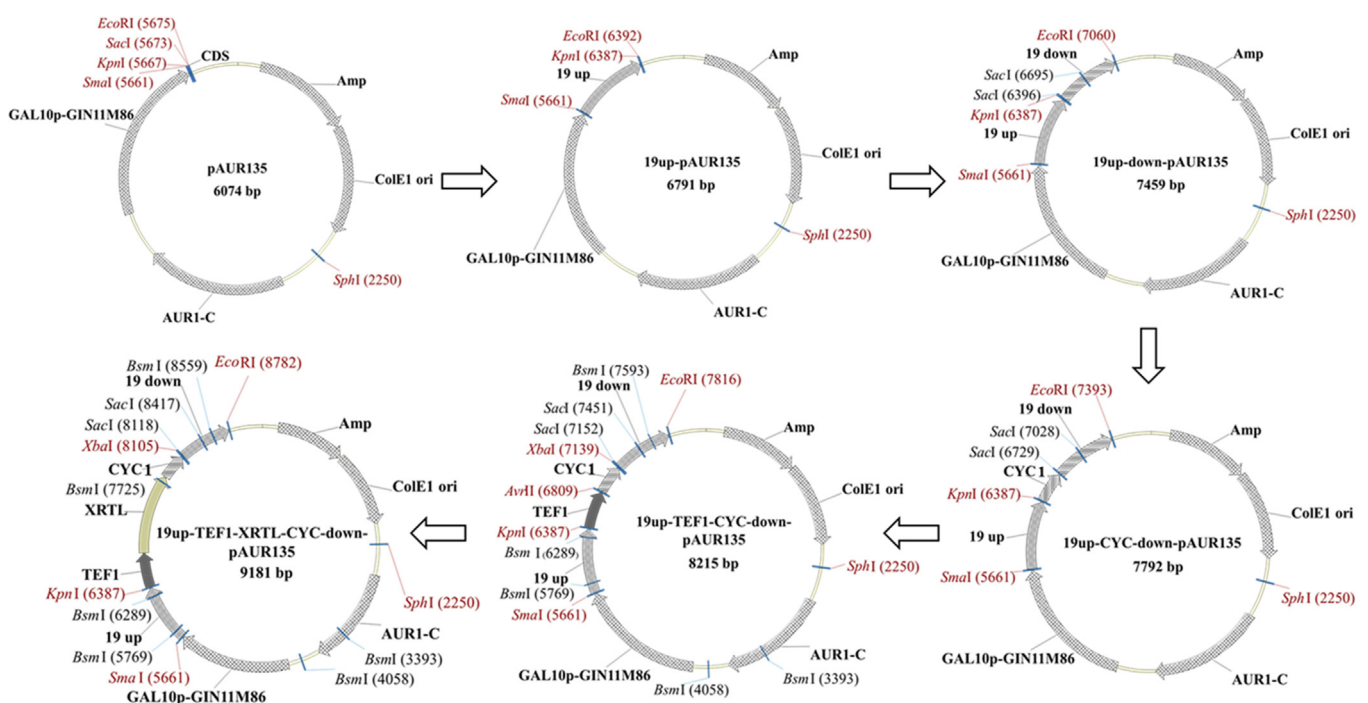


Fig. 1. Steps involved in the construction of recombinant 19up-*TEF1*-*XRTL*-*CYC*-down-pAUR135 expression plasmid. AUR1-C: Aureobasidin A resistant gene in *S. cerevisiae*; Amp: ampicillin resistance gene; GAL10p-GIN11M86: DNA sequence related to galactose-inducible growth inhibition in *S. cerevisiae*; ColE1 ori: origin of replication in *E. coli*.

defined as the amount of enzyme catalyzing the oxidation of 1 μmol of NADPH per minute at the assay conditions.

2.5. Characterization of recombinant XRTL

2.5.1. Effect of pH and temperature and the thermal denaturation kinetics

To study the effect of pH on the enzyme, the activity was measured at 50 °C, using 100 mM sodium citrate (pH 4.0–5.5); potassium phosphate (pH 6.0–8.0); and glycine-NaOH (pH 9.0–10). To determine the optimum temperature, the XRTL activity was measured between 30 °C and 80 °C at optimal pH. Thermostability and pH stability were investigated by incubating the enzyme at 40–70 °C in 20 mM phosphate buffer (pH 7) and at pH 4–10 at 50 °C, respectively. Samples were withdrawn every 15 min to calculate the residual enzyme activities.

The thermal denaturation kinetics of XRTL was studied in the range of 50–70 °C using the standard first-order enzyme deactivation kinetics. Change in enthalpy (ΔH , kJ/mol), change in free energy (ΔG , kJ/mol), and change in entropy (ΔS , J/mol-K) for thermal denaturation of XRTL were determined by using the following equations (Eyring and Stearn, 1939):

$$k_d = \left(\frac{K_b T}{h} \right) e^{(-\Delta H/RT)} e^{(-\Delta S/RT)} \quad (1)$$

$$\Delta H = E_d - RT \quad (2)$$

$$\Delta G = -RT \ln \left(\frac{K_d h}{K_b T} \right) \quad (3)$$

$$\Delta S = \frac{(\Delta H - \Delta G)}{T} \quad (4)$$

where k_d = thermal inactivation rate constant; E_0 and E_t were the initial (at $t = 0$) and residual (at $t = t$) XRTL activities; (E_d) = activation energy for denaturation of XRTL; K_b [Boltzmann's constant (R/N)] = 1.38×10^{-23} J/K; h (Planck's constant) = 6.63×10^{-34} J s; N (Avogadro's number) = 6.02×10^{23} per mol and R (gas constant) = 8.314 J/mol-K.

2.5.2. Effect of metal ions, additives and salts on purified recombinant XRTL

The effects of metal ions (Ca^{2+} , Cu^{2+} , Fe^{2+} , Mg^{2+} , Mn^{2+} , and Zn^{2+}) and reducing agents (EDTA and DTT) were studied by determination of XRTL specific activity in the presence of three concentrations of these compounds (0.5, 1 and 2 mM). The experiments were done in triplicate under optimal conditions and activity without any additive was considered as 100%. Similarly, the effect of 0–1 M NaCl and KCl on XRTL activity was determined under optimal conditions and activity without any additive was considered as 100%.

2.6. Enzyme kinetics in the presence of different substrates and cofactors

Kinetic parameters of the purified recombinant XRTL were determined against D-erythrose, D-ribose, D-arabinose, D-xylose, D-lyxose, D-allose, D-altrose, D-glucose, D-mannose, L-gulose, D-idose, D-galactose, D-talose, fructose, sucrose, maltose, lactose, cellobiose and xylobiose by measuring the initial velocities at constant NADPH (0.15 mM) and different concentrations of substrates ranging from 5 to 175 mM. The specific activity data was used to estimate the kinetic constants by fitting to the Michaelis–Menten equation:

$$v_0 = \frac{V_{max} [S]}{[S] + K_m} \quad (5)$$

where V_{max} is the maximal velocity; K_m is the Michaelis-Menten constant; S is the substrate concentration, and v_0 is the mean initial velocity. The Michaelis-Menten model was also used to study the enzyme specificity against 20–200 μM NADPH and NADH (disodium salt) as the known cofactors.

2.7. Determination of inhibitory concentrations and inhibition mechanisms of lignocellulose-derived by-products (LDBs)

Previously reported representatives of lignocellulose-derived inhibitory compounds, ferulic acid, vanillin, formic acid, acetic acid, benzoic acid, coumaric acid, cinnamic acid and gallic acid, were used to evaluate their inhibitory effect on XRTL. Their half maximal inhibitory concentrations (IC_{50}) were determined by measuring XRTL activities at varying gradients of increasing LDBs concentrations at 50 °C, pH 6.5 (100 mM of Tris-HCl buffer). The potent phenolic and non-phenolic inhibitors were selected and their inhibition kinetics was studied using the standard mixed inhibition model of Michaelis–Menten equation:

$$v_0 = \frac{V_{max} [S]}{K_m \left(1 + \frac{[I]}{K_i} \right) + [S] \left(1 + \frac{[I]}{K_i} \right)} \quad (6)$$

K_i values were estimated by the nonlinear regression analysis of Graphpad Prism 6.0 (GraphPad Software, Inc.).

2.8. Xylitol production by recombinant *S. cerevisiae* Y294 with the XRTL gene

Shake-flask fermentations were performed to determine xylitol production by *S. cerevisiae* Y294 harbouring the XRTL gene (*S. cerevisiae* Y294-XRTL). Two pre-inoculation steps were used. During the first pre-inoculation step, a single colony of *S. cerevisiae* Y294-XRTL was grown in 25 ml YPD medium at 30 °C and 200 rpm. After 72 h, 1 ml of culture was transferred into 50 ml fresh SC minimal medium and incubated at 30 °C and 200 rpm. This secondary pre-inoculation culture (0.5 ml) were transferred into 50 ml of SC minimal medium with an additional 2% xylose (produced from sugarcane bagasse, data not shown). The initial cell concentration was the same as that of the controlled experiments with *S. cerevisiae* Y294 without XRTL gene. Glucose, xylose, and xylitol concentrations were determined by the LCMS-2020 liquid chromatography system (Shimadzu) using an Aminex HPX 87-H column (Bio-Rad) and an ELSD-LT II detector (Shimadzu). The samples on the column were eluted at 50 °C with water as the mobile phase, at a flow rate of 0.5 ml/min.

3. Results and discussion

3.1. Expression, production and purification of XRTL

The expression plasmids, XRTL-pPIC9K and 19up-TEF1-XRTL-CYC-down-pAUR135 were successfully constructed by subcloning the XRTL gene from *T. lanuginosus* into pPIC9K and 19up-TEF1-CYC-down-pAUR135 under control of the AOX1 and TEF1 promoters, respectively. *P. pastoris* GS115 was used as a host for extracellular expression of the XRTL protein for characterization and purification purposes as purification allowed testing of xylose reductase activity on the absence of host aldo-keto reductase or its isozymes, while *S. cerevisiae* Y294 was used to study the effect of intracellular expression of XRTL on xylitol production. The XRTL gene sequence was deposited in the NCBI gene bank with accession number MG437302.

The *P. pastoris* transformants grown on YPD plates containing 2 mg/ml Geneticin were selected for XRTL production. Maximum XRTL activity of 5.23 ± 0.21 U/ml was achieved after 96 h of methanol induction. The recombinant enzyme was purified to homogeneity with an overall 13.77-fold increase in specific activity, through conventional ammonium sulfate precipitation (29.76 U/mg), ion-exchange chromatography (55.61 U/mg) and gel filtration chromatographic (78.06 U/mg) steps. The purified protein had an apparent molecular mass of ~39 kDa on SDS-PAGE gels (Fig. 2) and appears to migrate as a monomer during Superdex gel filtration chromatography (data not shown). A slightly higher molecular weight than the theoretically-

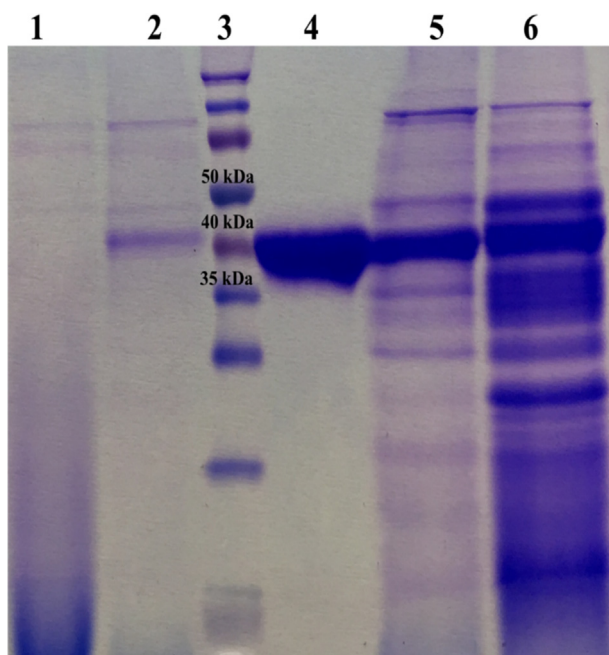


Fig. 2. SDS-PAGE analysis of XRTL-pPIC9K expressed in *P. pastoris* after protein purification. Lane 1: supernatant of *P. pastoris* GS115 transformed with pPIC9K; Lane 2: supernatant of *P. pastoris* GS115 transformed with XRTL-pPIC9K; Lane 3: Spectra multicolour broad range protein ladder; Lane 4: purified recombinant xylose reductase after gel filtration chromatography; Lane 5: eluent fraction of anion exchange chromatography; Lane 6: ammonium sulphate precipitation fraction.

predicted molecular weight of 36.74 kDa indicates possible glycosylation of the protein during the secretion process in *P. pastoris*. In this study, three potential N-glycosylation sites were identified at positions 26, 142 and 168 of XRTL using the NetNGlyc 1.0 Server (Blom et al., 2004).

3.2. Characterization of XRTL

Purified XRTL demonstrated activity in a broad range of pH (4.0–9.0) and temperature (30–70 °C). The enzyme was optimally active at pH 6.5 and exhibited remarkable stability at pH 6 and 7. It retained 58.7%, 73.76% and 45.95% activity after 30 min at pH 5, pH 8 and pH 9, respectively. However, the activity at pH 5 and pH 8 declined to 27% and 54%, respectively, after an incubation of 60 min. The half-life ($t_{1/2}$) at pH 5, 8 and 9 were 34.56 min, 69.14 min and 22.98 min, respectively. These results indicated that XRTL was more stable in alkaline condition than acidic conditions. The optimum pH and pH stability of XRTL was similar to other known xylose reductases (Dasgupta et al., 2016; Kumar and Gummadi, 2011). XRTL exhibited high stability at neutral pH and similar pH stability profiles were observed for other xylose reductases. The reason for these xylose reductases showing similar pH stability profiles could be that xylose reductase is an intracellular enzyme and the internal pH environment of cells is similar.

XRTL showed optimum activity at 50 °C, which is much higher than the optimum (37 °C) of the only reported xylose reductase from another

thermophilic fungus, *Talaromyces emersonii*, (Fernandes et al., 2009). Xylose reductase from *Neurospora crassa* (Woodyer et al., 2005) and *Rhizopus oryzae* (Zhang et al., 2015a) also showed optimal activities at 50 °C, similar to this study. The purified XRTL was extremely stable at 40 and 50 °C retaining 100% and 94.2% activity, respectively, after 120 min. The enzyme could only retain 24% activity at 60 °C, while the activity was completely lost when incubated at 70 °C for 45 min. Half-life ($t_{1/2}$) of purified XRTL at 50 °C, 55 °C and 60 °C were 1386 min, 49.86 min and 14.53 min, respectively. It is evident that the thermostability of XRTL is superior to the previously-reported xylose reductases from *R. oryzae*, *Debaryomyces nepalensis* NCYC 3413, *N. crassa* and *Kluyveromyces marxianus* NBRC 1777 which exhibited $t_{1/2}$ values of 83 min at 50 °C, 2.47 min at 50 °C, 94 min at 40 °C and 10 min at 42 °C, respectively (Malla and Gummadi, 2018; Woodyer et al., 2005; Zhang et al., 2011; Zhang et al., 2015a). Therefore, XRTL is the most thermostable xylose reductase reported thus far. Its high thermostability may be attributed to the presence of a high number of alanine residues (39 aromatic residues). Alanine has been considered as the best helix-forming residue in thermophiles (Kumwenda et al., 2013).

Although there is a plethora of data available on thermal deactivation kinetics of various enzymes, very limited information is available on the kinetics of microbial xylose reductases. Study of the thermal deactivation kinetics of XRTL resulted in positive values of all thermodynamic parameters (Table 1). The high positive ΔH values decreased slightly when the temperature was increased from 50 to 70 °C. This infers structural stability of the protein due to strong covalent bonds. Gibbs free energy (ΔG) of activation for XRTL denaturation decreased when temperature was increased from 50 to 60 °C, denoting the decreasing stability of this enzyme at higher temperatures. A slight increase in the value of ΔG from 60 to 70 °C was primarily entropy-driven and associated with the concomitant decrease in ΔS value, indicating that XRTL tends to defy disorders before the onset of unfolding, as with many thermostable enzymes (Siddiqui, 2017). More recently, Malla and Gummadi (2018) reported an enthalpy-driven thermal deactivation of mesophilic xylose reductase from *D. nepalensis* NCYC 3413 showing negative ΔH and ΔG values and a positive ΔS value.

Marked inhibition of XRTL activity was observed in the presence of 2 mM Cu^{2+} and Fe^{2+} ions (Table 2). Another transition metal ion, Zn^{2+} , also emerged as a potent inhibitor at 0.5 mM, 1 mM and 2 mM when it reduced the basal XRTL activity by 69%, 50% and 80%, respectively. The strong inhibitory potential of Cu^{2+} , Fe^{2+} and Zn^{2+} was also observed in other known xylose reductases (Kumar and Gummadi, 2011; Lee et al., 2003; Paidimuddala et al., 2017a). Kumar and Gummadi (2011) suggested a Cu^{2+} -mediated site-specific oxidation and a Fe^{2+} -mediated reduction as possible mechanisms for inhibition of xylose reductases. The other divalent metal-ions used in this study could only show a slight inhibition at all concentrations. No significant effect on XRTL activity was observed in the presence of EDTA, which suggests that XRTL is a metal-free enzyme. Similar observations were also reported in xylose reductases from *Candida parapsilosis* (Lee et al., 2003) and *D. nepalensis* NCYC 3413 (Kumar and Gummadi, 2011). The reducing agent, dithiothreitol (DTT) inhibited XRTL activity as observed previously in the xylose reductases from *D. nepalensis* NCYC 3413 (Kumar and Gummadi, 2011). In contrast, addition of DTT significantly enhanced the activity of xylose reductase from *K. marxianus* NBRC1777 (Zhang et al., 2011).

Table 1

Estimated thermodynamic parameters of thermal deactivation of purified XRTL at different temperatures.

Temperature (K)	k_d (min^{-1})	$t_{1/2}$ (min)	ΔH (kJ mol^{-1})	ΔG (kJ mol^{-1})	ΔS (kJ mol^{-1})
323.15	0.0005	1386	216.00	99.78	359.66
328.15	0.0139	49.856	215.96	92.298	376.87
333.15	0.0477	14.528	215.92	90.33	376.99
343.15	0.0818	8.472	215.84	91.58	362.10

Table 2
Effect of 0.5 mM, 1 mM and 5 mM divalent metal ions and reducing agents on the activity of XRTL.

Additives	Specific activity (U/mg)		
	0.5 mM	1 mM	2 mM
Metal ions			
Ca ²⁺	70 ± 2.5	62 ± 1.1	55 ± 2.8
Cu ²⁺	68 ± 1.9	65 ± 2.2	4 ± 0.3
Fe ²⁺	71 ± 2.5	67 ± 1.3	24 ± 1.7
Mg ²⁺	74 ± 2.2	70 ± 2.8	63 ± 1.5
Mn ²⁺	70 ± 1.8	68 ± 2.3	59 ± 2.0
Zn ²⁺	52 ± 2.3	38 ± 1.3	15 ± 1.3
Reducing agents			
EDTA	75 ± 1.21	72 ± 2.1	69 ± 1.6
DTT	68 ± 1.0	58 ± 1.3	51 ± 0.8
Control	75 ± 1.7		

Purified XRTL was highly tolerant to monovalent cations (Na⁺ and K⁺). It retained 85% and 80% of its activity in the presence 100 mM NaCl and KCl, respectively. About 45% of activity was retained at 600 mM of Na⁺ and K⁺, with residual activities of 33.72 ± 1.28 and 35.31 ± 0.86 U/mg, respectively. XRTL was more tolerant to Na⁺ than the other moderately halotolerant xylose reductase reported by Kumar and Gummadi (2011). The xylose reductase from *D. nepalensis* could only retain 15% of activity in the presence of 500 mM NaCl. Higher composition of acidic amino acids (12.42%) than basic amino acids (10.56%) could be the reason for higher halotolerance of XRTL.

3.3. Substrate specificity and coenzyme preference

HPLC analysis of the reaction mixture containing 1 mM xylose confirmed reductase activity of the purified protein by the conversion of xylose to xylitol. To test XRTL affinity towards other sugars, its preference to NADH and NADPH was studied. Purified XRTL exhibited dual coenzyme specificity for both NADH and NADPH, however, the protein preferred NADPH as indicated from a 3.68-times lower K_m value for NADPH than NADH (Table 3). Also, XRTL exhibited 66.8-fold higher catalytic efficiency towards NADPH than NADH. Evidently, the specific activity of XRTL with xylose as substrate and NADPH as coenzyme was 78 U/mg, while it showed a specificity activity of 2.68 U/mg with NADH as the coenzyme. This dual coenzyme utilization with preference for NADPH was also reported in many other xylose reductases (Fernandes et al., 2009; Kumar and Gummadi, 2011). The broad substrate specificity of purified XRTL is apparent and kinetic parameters are shown in Table 3. XRTL showed higher affinity and catalytic efficiency towards pentoses than hexoses. However, the highest affinity (K_m), turnover number (K_{cat}) and catalytic efficiency (K_{cat}/K_m) of the purified enzyme was observed towards erythrose at 10.07 mM, 10,101 per min and 1003.08 mM/min, respectively. Neuhauser et al. (1997) also reported erythrose as the most preferred substrate for xylose reductase from *Candida tenuis*, but xylose reductase from *C. parapsilosis* (Lee et al., 2003) showed lower catalytic efficiency and affinity towards erythrose than xylose. All attempts to use lyxose, mannose, talose, fructose, sucrose, maltose, lactose, cellobiose and xylobiose as alternative substrates in the presence of NADPH or NADH failed. Different xylose reductases from different sources show entirely different substrates preferences. While xylose reductase from *D. nepalensis* NCYC 3413 (Kumar and Gummadi, 2011) could not show activity against mannose, it was accepted as substrate for xylose reductase from *Candida intermedia* (Nidetzky et al., 2003). Similarly, fructose – A ketonic monosaccharide, acted as substrate for xylose reductase from *C. parapsilosis* (Lee et al., 2003), but not for xylose reductase from *N. crassa* (Woodyer et al., 2005). The disaccharide sucrose served as a substrate for xylose reductase from *Debaryomyces hansenii* (Biswas et al., 2012), but not for xylose reductase from *N. crassa* (Woodyer et al., 2005). In

Table 3
Apparent kinetic parameters of purified XRTL for NADPH-dependent reduction of different sugars and cofactor preference.

Substrate	V _{max} (μmol/mg/min)	K _m (mM)	K _{cat} (per min)	K _{cat} /K _m (mM/min)
D-Erythrose	76.79 ± 0.54	10.07 ± 0.33	10101 ± 100	1003.08
D-Ribose	79.54 ± 1.16	39.13 ± 1.74	10463 ± 180	267.39
D-Arabinose	88.48 ± 1.50	64.2 ± 2.69	11639 ± 233	181.29
D-Xylose	88.61 ± 1.27	15.36 ± 0.89	11656 ± 236	758.85
D-Lyxose	ND [*]	ND	ND	ND
D-Allose	9.459 ± 0.33	77.15 ± 5.30	1244 ± 59	16.12
D-Altrose	4.02 ± 0.17	101.1 ± 4.86	528.8 ± 22	5.23
D-Glucose	38.35 ± 1.67	222.4 ± 14.93	5045 ± 300	22.68
D-Mannose	ND	ND	ND	ND
D-Gulose	29.84 ± 3.418	349 ± 54.53	3925 ± 633	11.25
D-Idose	2.62 ± 0.13	30.95 ± 3.86	344.2 ± 16	11.12
D-Galactose	71.29 ± 2.47	101.7 ± 7.23	9378 ± 459	92.21
D-Talose	ND	ND	ND	ND
Fructose	ND	ND	ND	ND
Sucrose	ND	ND	ND	ND
Maltose	ND	ND	ND	ND
Lactose	ND	ND	ND	ND
Cellobiose	ND	ND	ND	ND
Xylobiose	ND	ND	ND	ND
Cofactors[#]	V _{max} (μmol/mg/min)	K _m (μM)	K _{cat} (per min)	K _{cat} /K _m (μM/min)
NADPH	94.43 ± 2.24	30.44 ± 2.69	12281 ± 129	403.45
NADH	5.14 ± 0.13	112.1 ± 6.02	676.7 ± 17.37	6.04

* ND: not detectable.

[#] Kinetic parameters with NADPH and NADH were calculated using 1 mM xylose as substrate

this study, no detectable activity was observed with fructose and tested disaccharides. This indicates that XRTL may only catalyze the reduction of aldehydic monosaccharides. Comparative kinetic studies of XRTL towards monosaccharides having R-configured hydroxyl groups at C-2 with the corresponding C-2 epimers (D-ribose vs. D-arabinose; D-allose vs D-altrose), showed that the OH group at the C2(R) position resulted in higher catalytic efficiency and affinity than OH group at C2(S) position. These present results are consistent with xylose reductase from *C. intermedia* (Nidetzky et al., 2003) and *Cryptococcus flavus* (Mayr et al., 2003) where the OH group at the C2(R) was preferred for enzyme activity. However, xylose reductase from *D. hansenii* binds sugars promiscuously and the C2(R) hydroxyl group does not contribute to the specificity of ligands binding to this enzyme (Biswas et al., 2012). XRTL showed high catalytic efficiency and affinity toward sugars having hydroxyl group at C2(R) and C3(S), but no detectable activities were observed with their corresponding C-3 epimers (D-xylose vs D-lyxose; D-glucose vs D-mannose; D-galactose vs D-talose). Interestingly, R-configured hydroxyl groups, when both present at C-2 and C-3 positions, do not favour the activity of XRTL. This has not been reported previously from all aldose reductases. Recombinant XRTL exhibited unique substrate specificity and kinetic characteristics as compared to other reported xylose reductases. This may be attributed to an extended loop (residue 314 to residue 318) at the C-terminal of XRTL, which has been shown to be important for substrate recognition in other AKR proteins (Yamamoto et al., 2016). The phylogenetic analysis clearly indicated that XRTL evolved from diverse ancestors to well-known yeast and filamentous fungal xylose reductases (Fig. 3).

3.4. Inhibition kinetics of XRTL due to LDBs

During pretreatment of lignocellulosic biomass, phenolic compounds are the major by-products that inhibit microbial and enzymatic biocatalysts (Jönsson and Martín, 2016). Among the tested plant-derived phenolic compounds, ferulic acid exhibited highest inhibitory effect on XRTL with an IC₅₀ of 0.055 mM. This was followed by vanillin (IC₅₀ of 0.149 mM), coumaric acid (IC₅₀ of 3.612 mM), cinnamic acid

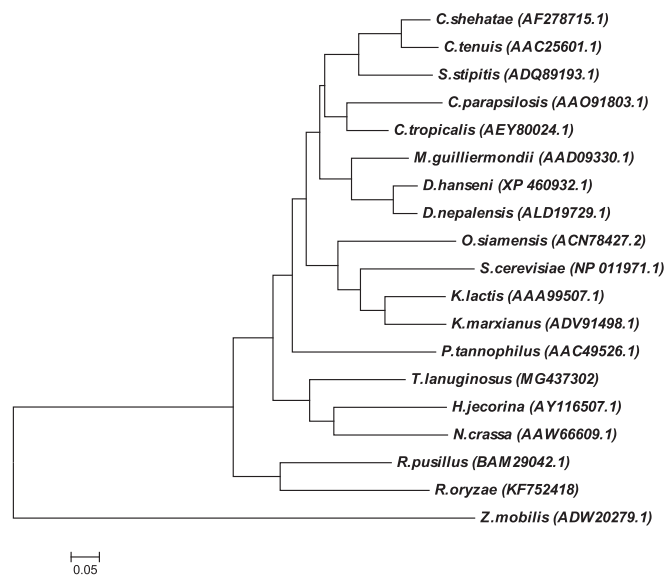


Fig. 3. Phylogenetic analysis of XRTL amino acid sequence with existing xylose reductases. The analysis was done using the neighbour-joining method available with MEGA7.0 software. The NCBI accession numbers of xylose reductases have been provided after the name of each microbial source.

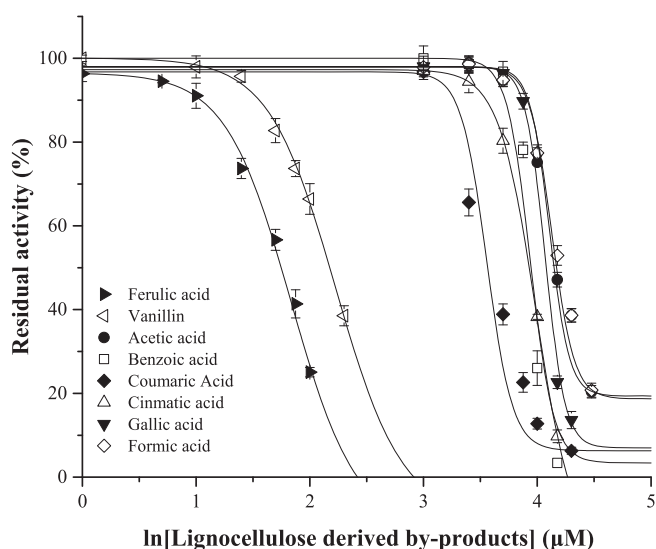


Fig. 4. Residual activity at different concentration of lignocellulose derived by-products (LDBs). The concentrations of LDBs were expressed in terms of natural logarithm.

Table 4
Kinetic parameters of XRTL in the presence of various LDBs.*

LDB	Concentration (mM)	V_{max} (U/mg)	K_m (mM)	K_i (mM)	Inhibition mechanism
Control†	–	88.61 ± 1.62	15.36 ± 1.14	–	
Ferulic acid	0.025	67.05 ± 1.65	30.72 ± 2.36		
	0.05	56.58 ± 1.93	37.98 ± 3.71	0.015 ± 0.002	Mixed
	0.06	45.94 ± 1.56	52.71 ± 4.58		
Vanillin	0.05	82.39 ± 2.50	30.31 ± 2.87		
	0.1	78.06 ± 2.20	38.57 ± 3.10	0.042 ± 0.003	Mixed
	0.15	65.89 ± 2.23	76.82 ± 5.59		
Acetic acid	10	76.14 ± 2.13	44.36 ± 3.33		
	15	64.53 ± 2.20	57 ± 4.72	3.75 ± 0.59	Mixed
	20	52.43 ± 1.72	73.24 ± 5.28		

* LDB: lignocellulose-derived by-products; K_m : Michaelis-Menten constant; V_{max} : maximal velocity; K_i : inhibition constant.

† Controlled experiments were performed without any LDBs in the reaction mixture.

(IC_{50} of 8.15 mM), benzoic acid (IC_{50} of 8.785 mM) and gallic acid (IC_{50} of 12.27 mM). The non-phenolic compounds, acetic acid and formic acid were the least potent inhibitors with IC_{50} values of 15.62 mM and 16.36 mM, respectively (Fig. 4).

Higher enzyme inhibition by phenolic compounds may be attributed to the presence of hydroxyl and carbonyl groups as reported recently by Zhai et al. (2018). However, in contrast to their findings where the authors reported highest inhibition by smaller molecular weight compound, this study showed strongest inhibition by a phenolic compound with highest molecular weight among the tested inhibitors (ferulic acid, 194.19 g/mol). This can be due to steric hindrance caused by feruloylation of the substrate and/or the enzyme and/or the enzyme-substrate complex.

Gallic acid (IC_{50} of 12.27 mM) and acetic acid (IC_{50} of 15.62 mM) were more inhibitory to XRTL than the xylose reductase from *D. nepalensis*, where IC_{50} values were reported as 40 mM and 60 mM, respectively (Paidimuddala et al., 2017b). However, inhibition by vanillin on xylose reductase from *D. nepalensis* was similar to the present study, with an IC_{50} value of 0.14 mM. Acetic acid showed much less of an effect on crude xylose reductase from *Candida tropicalis* with an IC_{50} of 190 mM (Rafiqul et al., 2015).

To understand the mechanism of inhibition, the enzyme kinetics of XRTL was investigated in the presence of three different concentrations of ferulic acid, vanillin and acetic acid in separate experiments. As the concentrations of ferulic acid was increased, K_m values increased from 15.36 ± 1.14 to 52.71 ± 4.58 mM and V_{max} values decreased from 88.61 ± 1.62 to 45.94 ± 1.56 U/mg (Table 4). This suggested that ferulic acid inhibits XRTL by the mechanism of mixed inhibition. Similar patterns of mixed inhibition of XRTL were also observed for vanillin and acetic acid. The K_i values of ferulic acid, vanillin and acetic acid were estimated to be 0.015, 0.042 and 3.75 mM, respectively (Table 4). Ferulic acid showed a strong inhibitory effect with lowest K_i values. This is the first report on ferulic acid showing strong inhibition towards a xylose reductase.

3.5. Xylitol production by recombinant *S. cerevisiae* Y294 with the XRTL gene

XRTL was successfully expressed in *S. cerevisiae* Y294 with an activity of 0.22 U/mg activity in the crude cell extract. Xylitol cannot be efficiently metabolized by *S. cerevisiae*, so xylose conversion requires the simultaneous metabolism of a co-substrate such as glucose and ethanol for continuous regeneration of NAD(P)H and generation of maintenance energy. *S. cerevisiae* Y294 and *S. cerevisiae* Y294-XRTL were cultured in SC minimal medium with 2% glucose and xylose (Fig. 5). Immediately after inoculation, both strains consumed glucose and concomitantly produced biomass. The biomass formation was halted and glucose was completely consumed after 24 h. Xylose depletion and xylitol production was then detected. The xylose reduction

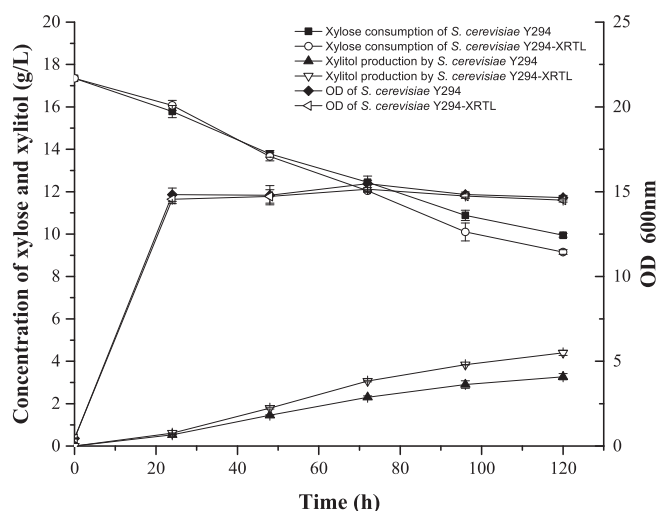


Fig. 5. Growth and xylitol fermentation profiles of *S. cerevisiae* Y294 versus recombinant *S. cerevisiae* Y294-XRTL in SC minimal medium without pH adjustment.

and xylitol formation slowed slightly after 100 h incubation. *S. cerevisiae* Y294-XRTL which contained a single copy of XRTL in its chromosome, showed xylitol production of 4.4 ± 0.13 g/L after 120 h incubation, about 34% higher than that of *S. cerevisiae* Y294 without XRTL (3.27 ± 0.15 g/L).

S. cerevisiae is a promising candidate for industrial production of biofuels and value-added bio-chemicals from lignocellulosic biomass. High temperatures fermentation can effectively accelerate the rate of reaction, avoid or minimize microbial contamination, shorten microbial fermentation period and facilitate downstream product recovery. Therefore, many researchers have attempted to improve the thermotolerance of *S. cerevisiae* for ethanol and chemicals production (Benjaphokee et al., 2012; Xu et al., 2018). However, such strains still have low fermentation efficiency, possibly because the growth temperature is high and not compatible with the optimum temperature of the critical enzymes in the metabolic pathways. This decreases the protein stability and leads to lower metabolic rates. As *S. cerevisiae* does not have a specific xylose reductase, many researchers have attempted to express xylose reductases from mesophilic yeasts such as *Pichia stipitis*, *Candida* species and the *S. cerevisiae* *GRE3* gene (coding for a non-specific aldose reductase) in *S. cerevisiae*, mainly for lignocellulose bioconversion. However, enzyme activity and stability of those xylose reductase is not satisfactory at higher temperatures (Neuhauser et al., 1997; Zhang et al., 2011). Interestingly, xylose reductase from the thermotolerant yeast *K. marxianus* showed optimal activity only at 20 °C. Therefore, they are not suitable for construction of xylose metabolic pathways in thermotolerant *S. cerevisiae*. In this study, one copy of *XRTL* gene was integrated into the chromosome of *S. cerevisiae*, and it had a significant effect on xylose reductase activity and xylitol production. Kogje and Ghosalkar (2016) using a high copy number plasmid, overexpressed the *S. cerevisiae* *GRE3* gene and xylose reductase from *C. tropicalis* and *N. crassa* in *S. cerevisiae*. Xylitol production of *S. cerevisiae* harbouring the *GRE3* gene and xylose reductase gene from *C. tropicalis* was around 2 times more than the *S. cerevisiae* control. The *N. crassa* gene showed no significant effect on xylitol production. Kim et al. (1999) studied the effect of copy number of the *P. stipitis* xylose reductase in *S. cerevisiae* and showed that the xylose reductase activity was only 2.5 times higher when comparing a copy number of 30 to a single copy. Pratter et al. (2015) pointed out that xylose reductase activity did not correlate with the xylitol productivities and other factors limited xylose conversion in *S. cerevisiae*. By comparison, a single copy of *XRTL* caused a 1.70 times increase in enzyme activity and a 34% increase in xylitol production. This increase in xylitol production may

be attributed to the much higher affinity and catalytic rate of XRTL compared to other enzymes, since the intracellular environment is much more complex than the extracellular environment. XRTL has a low K_m resulting in efficient binding with xylose. Those results combined with the stability studies suggest that XRTL can be used as an efficient component for construction of a xylose metabolic pathway in *S. cerevisiae*, specifically in thermotolerant *S. cerevisiae* for the bio-conversion of xylose to value-added compounds.

4. Conclusions

In this study, a thermostable recombinant xylose reductase from *T. lanuginosus* SSBP was successfully expressed in *P. pastoris* and *S. cerevisiae*. The enzyme showed broad substrate specificity and preferred NADPH over NADH as the cofactor. The recombinant *S. cerevisiae* harbouring XRTL successfully produced xylitol. Future studies will be directed towards expressing the enzyme at high copy number to improve xylitol production. Additionally, co-crystallization of XRTL with potent inhibitors, substrates and cofactors will be helpful to identify key amino acid residues and develop a robust enzyme using site-directed mutagenesis.

Acknowledgements

The financial support from the National Research Foundation, Republic of South Africa and Durban University of Technology is gratefully acknowledged.

Appendix A. Supplementary data

Supplementary data to this article can be found online at <https://doi.org/10.1016/j.biortech.2019.02.102>.

References

- Benjaphokee, S., Hasegawa, D., Yokota, D., Asvarak, T., Auesukaree, C., Sugiyama, M., Kaneko, Y., Boonchird, C., Harashima, S., 2012. Highly efficient bioethanol production by a *Saccharomyces cerevisiae* strain with multiple stress tolerance to high temperature, acid and ethanol. *N. Biotechnol.* 29, 379–386.
- Biswas, D., Pandya, V., Singh, A.K., Mondal, A.K., Kumaran, S., 2012. Co-factor binding confers substrate specificity to xylose reductase from *Debaryomyces hansenii*. *PLoS One* 7, e45525.
- Blom, N., Sicheritz-Ponten, T., Gupta, R., Gammeltoft, S., Brunak, S., 2004. Prediction of post-translational glycosylation and phosphorylation of proteins from the amino acid sequence. *Proteomics* 4, 1633–1649.
- Bradford, M.M., 1976. A rapid and sensitive method for the quantitation of microgram quantities of protein utilizing the principle of protein-dye binding. *Anal. Biochem.* 72, 248–254.
- Dasgupta, D., Ghosh, D., Bandhu, S., Agrawal, D., Suman, S.K., Adhikari, D.K., 2016. Purification, characterization and molecular docking study of NADPH dependent xylose reductase from thermotolerant *Kluyveromyces* sp. IPE453. *Process Biochem.* 51, 124–133.
- Eyring, H., Stearn, A.E., 1939. The application of the theory of absolute reaction rates to proteins. *Chem. Rev.* 24, 253–270.
- Fernandes, S., Tuohy, M.G., Murray, P.G., 2009. Xylose reductase from the thermophilic fungus *Talaromyces emersonii*: cloning and heterologous expression of the native gene (*Texr*) and a double mutant (*Texr*^{K271R + N273D}) with altered coenzyme specificity. *J. Biosci.* 34, 881–890.
- Flagfeldt, D.B., Siewers, V., Huang, L., Nielsen, J., 2009. Characterization of chromosomal integration sites for heterologous gene expression in *Saccharomyces cerevisiae*. *Yeast* 26, 545–551.
- Jönsson, L.J., Martín, C., 2016. Pretreatment of lignocellulose: formation of inhibitory by-products and strategies for minimizing their effects. *Bioresour. Technol.* 199, 103–112.
- Jiang, Z., Zhao, P., Hu, C., 2018. Controlling the cleavage of the inter- and intra-molecular linkages in lignocellulosic biomass for further biorefining: a review. *Bioresour. Technol.* 256, 466–477.
- Kim, Y.S., Kim, S.Y., Kim, J.H., Kim, S.C., 1999. Xylitol production using recombinant *Saccharomyces cerevisiae* containing multiple xylose reductase genes at chromosomal δ -sequences. *J. Biotechnol.* 67, 159–171.
- Kogje, A., Ghosalkar, A., 2016. Xylitol production by *Saccharomyces cerevisiae* over-expressing different xylose reductases using non-detoxified hemicellulosic hydrolysate of corn cob. *3 Biotech* 6, 127.
- Kratzer, R., Wilson, D.K., Nidetzky, B., 2006. Catalytic mechanism and substrate selectivity of aldo-keto reductases: insights from structure-function studies of *Candida*

- tenuis* xylose reductase. IUBMB Life 58, 499–507.
- Kumar, S., Gummadi, S.N., 2011. Purification and biochemical characterization of a moderately halotolerant NADPH dependent xylose reductase from *Debaryomyces nepalensis* NCYC 3413. Bioresour. Technol. 102, 9710–9717.
- Kumwenda, B., Lithauer, D., Bishop, O.T., Reva, O., 2013. Analysis of protein thermostability enhancing factors in industrially important thermus bacteria species. Evol. Bioinform. Online 9, 327–342.
- Lee, J.K., Koo, B.S., Kim, S.Y., 2003. Cloning and characterization of the *xylI* gene, encoding an NADH-preferring xylose reductase from *Candida parapsilosis*, and its functional expression in *Candida tropicalis*. Appl. Environ. Microbiol. 69, 6179–6188.
- Looke, M., Kristjuhan, K., Kristjuhan, A., 2011. Extraction of genomic DNA from yeasts for PCR-based applications. Biotechniques 50, 325–328.
- Malla, S., Gummadi, S.N., 2018. Thermal stability of xylose reductase from *Debaryomyces nepalensis* NCYC 3413: deactivation kinetics and structural studies. Process Biochem. 67, 71–79.
- Mayr, P., Petschacher, B., Nidetzky, B., 2003. Xylose reductase from the basidiomycete fungus *Cryptococcus flavus*: purification, steady-state kinetic characterization, and detailed analysis of the substrate binding pocket using structure-activity relationships. J. Biochem. 133, 553–562.
- Mchunu, N.P., Permaul, K., Rahman, A.Y.A., Saito, J.A., Singh, S., Alam, M., 2013. Xylanase superproducer: genome sequence of a compost-loving thermophilic fungus *Thermomyces lanuginosus* strain SSBP. Genome Announc. 1 (3), e00388–e413.
- Medina, J.D.C., Woiciechowski, A.L., Zandoná, A., Brar, S.K., Magalhaes, A.L., Soccol, C.R., 2018. Energetic and economic analysis of ethanol, xylitol and lignin production using oil palm empty fruit bunches from a Brazilian factory. J. Clean. Prod. 195, 44–55.
- Neuhauser, W., Haltrich, D., Kulbe, K.D., Nidetzky, B., 1997. NAD(P)H-dependent aldose reductase from the xylose-assimilating yeast *Candida tenuis*. Isolation, characterization and biochemical properties of the enzyme. Biochem. J. 326, 683–692.
- Nidetzky, B., Bruggler, K., Kratzer, R., Mayr, P., 2003. Multiple forms of xylose reductase in *Candida intermedia*: comparison of their functional properties using quantitative structure-activity relationships, steady-state kinetic analysis, and pH studies. J. Agric. Food Chem. 51, 7930–7935.
- Paidimuddala, B., Aradhya, G.K., Gummadi, S.N., 2017a. A halotolerant aldose reductase from *Debaryomyces nepalensis*: gene isolation, overexpression and biochemical characterization. RSC Adv. 7, 20384–20393.
- Paidimuddala, B., Rathod, A., Gummadi, S.N., 2017b. Inhibition of *Debaryomyces nepalensis* xylose reductase by lignocellulose derived by-products. Biochem. Eng. J. 121, 73–82.
- Pratter, S.M., Eixelsberger, T., Nidetzky, B., 2015. Systematic strain construction and process development: xylitol production by *Saccharomyces cerevisiae* expressing *Candida tenuis* xylose reductase in wild-type or mutant form. Bioresour. Technol. 198, 732–738.
- Rafiqul, I.S.M., Sakinah, A.M.M., Zularisam, A.W., 2015. Inhibition by toxic compounds in the hemicellulosic hydrolysates on the activity of xylose reductase from *Candida tropicalis*. Biotechnol. Lett. 37, 191–196.
- Rao, L.V., Goli, J.K., Gentela, J., Koti, S., 2016. Bioconversion of lignocellulosic biomass to xylitol: an overview. Bioresour. Technol. 213, 299–310.
- Siddiqui, K.S., 2017. Defying the activity-stability trade-off in enzymes: taking advantage of entropy to enhance activity and thermostability. Crit. Rev. Biotechnol. 37, 309–322.
- Woodyer, R., Simurdiak, M., Van der Donk, W.A., Zhao, H., 2005. Heterologous expression, purification, and characterization of a highly active xylose reductase from *Neurospora crassa*. Appl. Environ. Microbiol. 71, 1642–1647.
- Xu, K., Gao, L.M., UL Hassan, J., Zhao, Z.P., Li, C., Huo, Y.X., Liu, G.Y., 2018. Improving the thermo-tolerance of yeast base on the antioxidant defense system. Chem. Eng. Sci. 175, 335–342.
- Yamamoto, K., Higashiura, A., Suzuki, M., Shiotsuki, T., Sugahara, R., Fujii, T., Nakagawa, A., 2016. Structural characterization of an aldo-keto reductase (AKR2E5) from the silkworm *Bombyx mori*. Biochem. Biophys. Res. Commun. 474, 104–110.
- Zhang, B., Zhang, L., Wang, D., Gao, X., Hong, J., 2011. Identification of a xylose reductase gene in the xylose metabolic pathway of *Kluyveromyces marxianus* NBRC1777. J. Ind. Microbiol. Biotechnol. 38, 2001–2010.
- Zhang, M., Jiang, S.T., Zheng, Z., Li, X.J., Luo, S.Z., Wu, X.F., 2015a. Cloning, expression, and characterization of a novel xylose reductase from *Rhizopus oryzae*. J. Basic Microbiol. 55, 907–921.
- Zhang, M., Puri, A.K., Govender, A., Wang, Z.X., Singh, S., Permaul, K., 2015b. The multi-chitinolytic enzyme system of the compost-dwelling thermophilic fungus *Thermomyces lanuginosus*. Process Biochem. 50, 237–244.
- Zhai, R., Hu, J., Saddler, J.J.N., 2018. Extent of enzyme inhibition by phenolics derived from pretreated biomass is significantly influenced by the size and carbonyl group content of the phenolics. ACS Sustain. Chem. Eng. 6, 3823–3829.